

**Figure S1. GI shares targets with light signaling components and interacts with PIF proteins, Related to Figure 1**

(A) Overlap between DEGs in *gi-2*, a comprehensive set of PIF-regulated genes, and DEGs in *cca1-1;lhy-11* mutants (GI-PIF intersection  $p < 2.2e-16$ ; GI-CCA1/LHY intersection  $p < 2.2e-16$ ).

(B and C) Phase enrichment heatmaps depicting the p-value of the phase of peak expression enrichment of genes differentially expressed in *gi-2* only (GI), regulated by PIFs only (PIFs), and potentially regulated by both GI and PIFs (GI-PIFs) (B) or DEGs in *gi-2* only (GI), *cca1-1;lhy-11* only (CCA1;LHY), and in both *gi-2* and *cca1-1;lhy-11* (GI/CCA1;LHY) (C) under 12h light and 12h dark conditions (\* $p < 0.01$ ). Day period is marked in yellow and night period in gray.

(D) Heat map showing the GO term enrichment scores of genes differentially expressed in *gi-2* only (GI), potentially regulated by both GI and PIFs (GI-PIFs), and differentially expressed in both *gi-2* and *cca1-1;lhy-11* (GI-CCA1/LHY).

(E) Hypocotyl length measurements from wildtype (Col-0) and *gi-2* seedlings grown for 6 days under different light conditions (in gray, mean  $\pm$  SEM,  $n=20-36$ ; \*\*\* $p < 0.001$  Student's *t*-test). D, darkness; cR, constant red light ( $1 \mu\text{mol m}^2\text{s}^{-1}$ ); cB, constant blue light ( $1 \mu\text{mol m}^2\text{s}^{-1}$ ); SD, short day photoperiod (8h light, 16h dark).

(F, G) Yeast two-hybrid (Y2H) assays showing interaction of GI and PIF proteins. Bait and prey constructs were co-transformed into yeast cells. SD-WL, minimal medium lacking Trp and Leu; SD-WLH, selective medium lacking Trp, Leu and His, which was supplemented with 50 mM 3AT; X-gal, qualitative  $\beta$ -galactosidase activity results obtained from the X-gal assay. (G) Quantitation of  $\beta$ -galactosidase activity (Miller units) for every pair of bait and prey proteins indicated ( $n=4$ ). Values represent means  $\pm$  SEM. Statistically significant differences between mean values by Student's *t*-test relative to the pExpAD502 control vector are shown (\*\* $p < 0.01$ , \*\*\* $p < 0.001$ ).

(H) *In vitro* pull-down assays performed to map the interaction domains between GI and PIF3. Proteins were expressed in a TnT *in vitro* expression system and immunoprecipitated with anti-HA antibody. The recovered fractions were analyzed by Western blot using anti-Flag and anti-HA antibodies. A scheme of the deleted protein versions is shown on the upper panel.

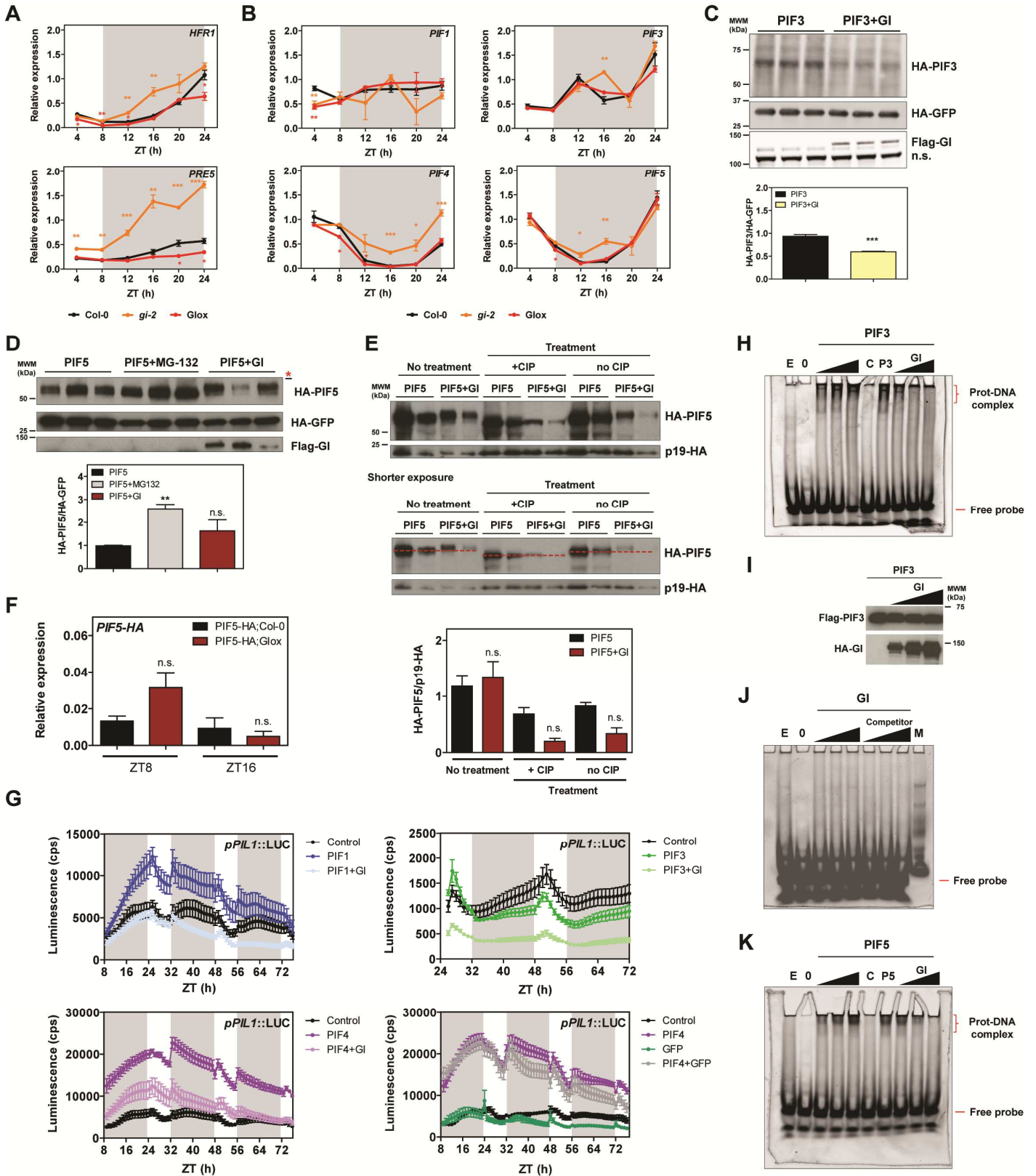


## Figure S2. GI modulates PIF stability and activity, Related to Figure 2

(A and B) Relative expression of *HFR1* and *PRE5* (A) and *PIF1*, *PIF3*, *PIF4*, and *PIF5* (B) in wildtype (Col-0), *gi-2*, and Glox seedlings grown for 10 days in SDs (mean  $\pm$  SEM of 3 biological replicates). White and gray shadings represent day and night, respectively.

(C and D) HA-PIF3 (C) and HA-PIF5 (D) accumulation in *N. benthamiana* leaves in the presence or absence of Flag-GI. Protein levels were normalized against HA-GFP levels. Western blot quantitation is shown on the respective lower panels. Values represent mean  $\pm$  SEM (n=3).

(E) Western blot analysis of the treatment with calf intestinal alkaline phosphatase (CIP) of PIF5-HA expressed in *N. benthamiana* leaves in the presence and absence of GI. Western blot quantitation is shown on the lower panel. Values represent mean  $\pm$  SEM (n=2).

(F) Relative expression of the *PIF5-HA* transgene in wildtype (Col-0) and Glox plants at ZT8 and 16 in SDs (mean  $\pm$  SEM of 3 biological replicates).

(G) Transactivation assays in *N. benthamiana* leaves. Different effectors were co-expressed with the *pPIL1::LUC* reporter construct. Luminescence was measured 2 days post-infiltration in SD conditions. Results show mean  $\pm$  SEM (n=12).

(H, J and K) EMSA studies using a *PIL1* promoter fragment containing two G-boxes as probe. Flag-PIF3 (H), HA-GI (H,J,K), and Flag-PIF5 (K) were expressed in an *in vitro* transcription and translation system. The Cy5 labeled DNA probe was incubated with increasing amounts of the proteins as indicated (1, 2, 4  $\mu$ l) or with the maximal amount of protein and increasing quantities of unlabeled probe (50, 100, 200 fold excess) (competitor, C). E, control incubation with 4  $\mu$ l extract without expressed protein. 0, incubation without extract. M, molecular weight marker. (H and K) The binding of Flag-PIF3 and Flag-PIF5 to the probe was additionally analyzed in the presence of increasing quantities of HA-GI (1, 2, 4  $\mu$ l).

(I) Western blot analysis of Flag-PIF3 stability in the presence of increasing quantities of HA-GI (1, 2, 4  $\mu$ l) during the binding reactions.

(A-F) n.s. not significant, \* $p < 0.05$ , \*\* $p < 0.01$ , \*\*\* $p < 0.001$  Student's *t*-test.

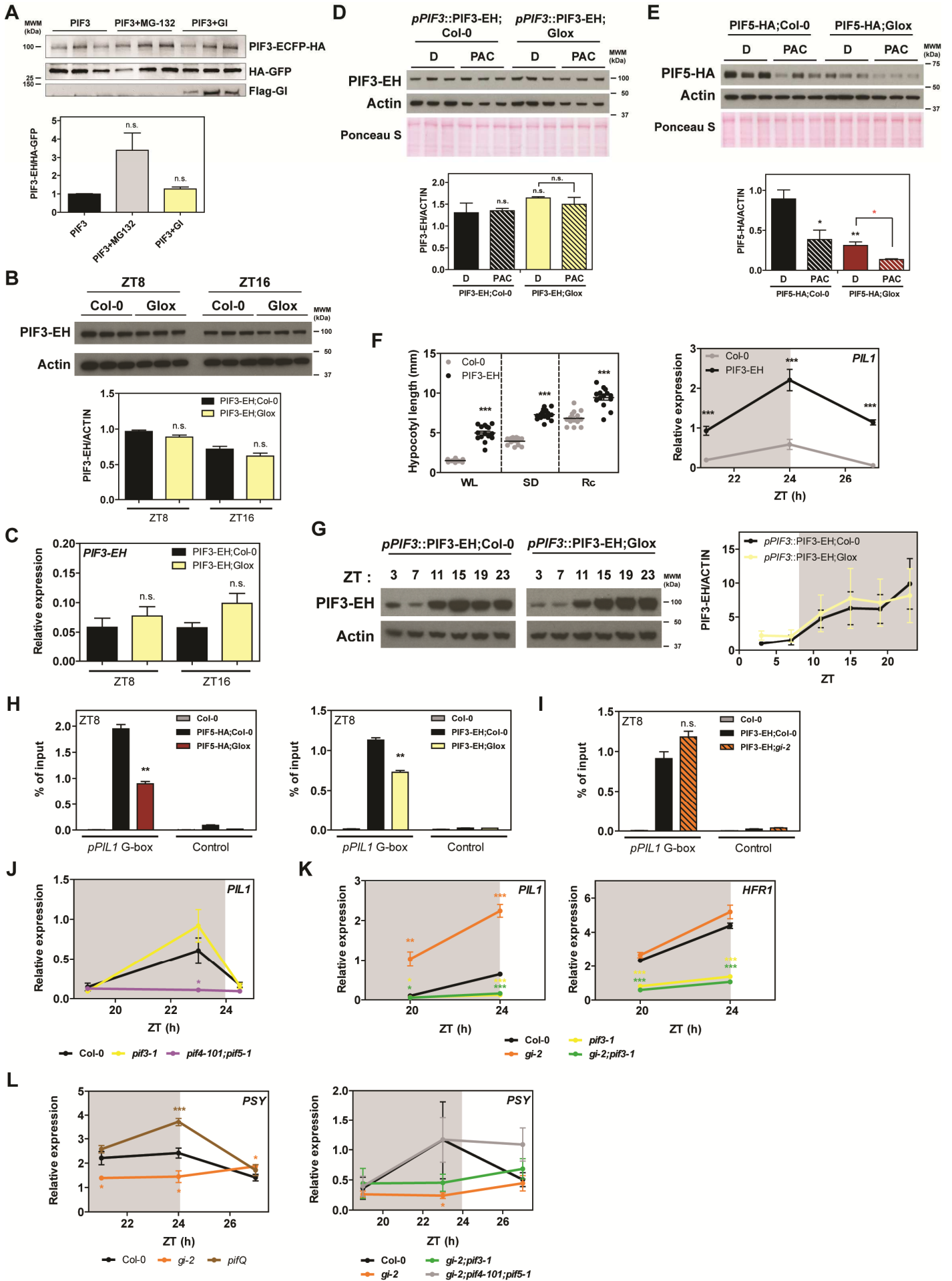


### Figure S3. GI modulates PIF stability and activity, Related to Figure 2

(A) HA-PIF3 accumulation in *N. benthamiana* leaves treated with 25  $\mu$ M MG-132 or in the presence of Flag-GI. Protein levels were normalized against HA-GFP levels. Western blot quantitation is shown on the lower panel. Values represent mean  $\pm$  SEM (n=3).

(B) PIF3-ECFP-HA protein accumulation at ZT8 and 16 in the indicated backgrounds under SD conditions. Protein levels were normalized against ACTIN levels. The quantitation is shown on the lower panel (mean  $\pm$  SEM of 3 biological replicates).

(C) Relative expression of the *PIF3-ECFP-HA* transgene in wildtype (Col-0) and Glox plants at ZT8 and 16 in SDs (mean  $\pm$  SEM of 3 biological replicates).

(D and E) PIF3-ECFP-HA (D) and PIF5-HA (E) accumulation in Col-0 and Glox plants in etiolated seedlings grown for 3 days with (PAC) or without (D) 1 $\mu$ M paclobutrazol. Protein levels normalized against ACTIN levels. The quantitations are shown on the respective lower panels. Values represent mean  $\pm$  SEM (n=3).

(F) Physiological characterization of PIF3-ECFP-HA overexpression lines. Left panel, hypocotyl length measurements (n=14-17) from wildtype (Col-0) and PIF3-ECFP-HA seedlings grown for 7 days in constant white light (WL), SDs (SD) or for 3 days in constant red light (Rc, 10  $\mu$ mol m<sup>2</sup>s<sup>-1</sup>). Right panel, relative expression of *PIL1* in wildtype (Col-0) and PIF3-ECFP-HA seedlings at the indicated ZTs in SDs (mean  $\pm$  SEM of 3 biological replicates).

(G) Representative western blots showing the accumulation of PIF3-ECFP-HA across a SD photo-cycle in the wildtype background (Col-0) and in Glox plants. Expression of PIF3-ECFP-HA in these lines is driven by the *PIF3* endogenous promoter. Protein levels were determined with anti-HA antibody and ACTIN levels were used as loading control. Western blot quantitation is shown on the right panel (mean  $\pm$  SEM, n=3 biological replicates).

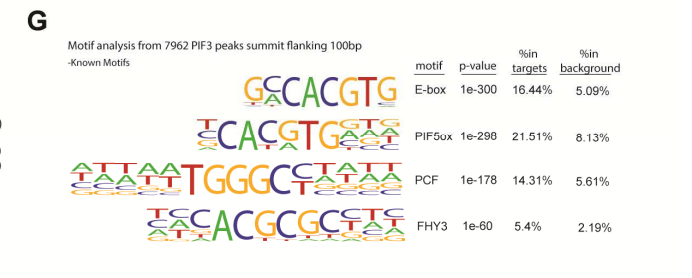
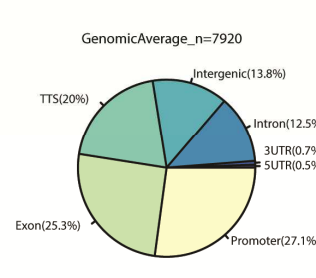
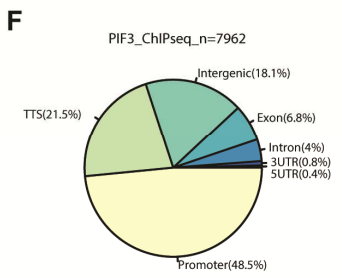
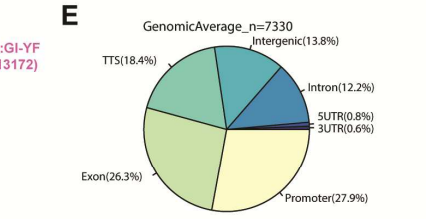
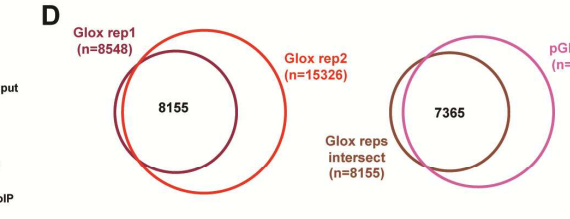
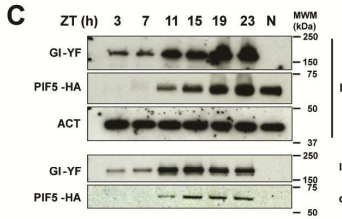
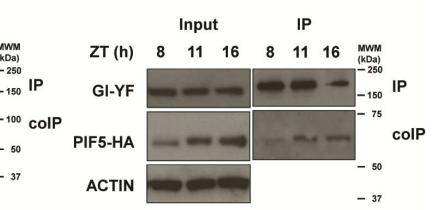
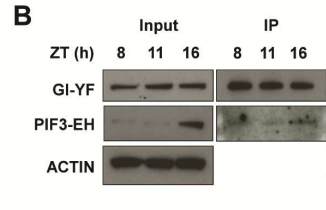
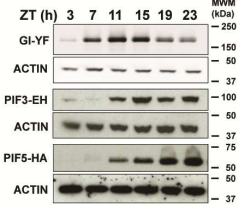
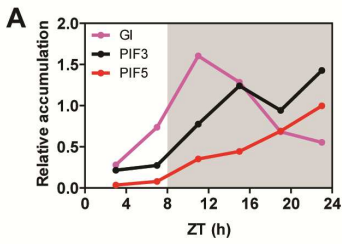
(H and I) ChIP assays of 10-day-old seedlings grown in SD conditions and harvested at ZT8 in the indicated lines. The enrichment of the specified regions in the immunoprecipitated samples was quantified by qPCR. Values represent mean  $\pm$  SEM (n=2-4).

(J) Relative expression of *PIL1* in the indicated backgrounds and ZTs in SDs (mean  $\pm$  SEM of 3 biological replicates). White and gray shadings represent day and night, respectively.

(K) Relative expression of *PIL1* and *HFR1* was additionally analyzed in 3 day old seedlings of the indicated backgrounds in SDs (mean  $\pm$  SEM of 3 biological replicates).

(L) Relative expression of *PSY* in the indicated backgrounds and ZTs in SDs (mean  $\pm$  SEM of 3 biological replicates). White and gray shadings represent day and night, respectively.

(A-L) n.s. not significant, \*p<0.05, \*\*p<0.01, \*\*\*p<0.001 Student's *t*-test.



**H**

GO biological process complete	Enrichment
ethylene-activated signaling pathway	23,397
abscisic acid-activated signaling pathway	16,793
brassinosteroid mediated signaling pathway	15,492
response to salicylic acid	14,191
auxin-activated signaling pathway	13,924
jasmonic acid mediated signaling pathway	8,695
cytokinin-activated signaling pathway	8,695
gibberellin mediated signaling pathway	7,439
hormone biosynthetic process	7,437
positive regulation of abscisic acid-activated signaling	7,304
regulation of hormone metabolic process	7,112
auxin polar transport	6,470
regulation of growth	12,507
floral organ development	10,238
leaf senescence	9,506
axis specification	7,726
floral whorl development	7,488
adaxial/abaxial pattern specification	7,105
positive regulation of post-embryonic development	7,101
cellular developmental process	6,822
meristem development	6,812
lateral root morphogenesis	6,838
anatomical structure arrangement	6,643
negative regulation of seed germination	6,348
stomatal complex morphogenesis	6,092
regulation of leaf senescence	6,053
shade avoidance	9,226
red or far-red light signaling pathway	7,168
response to red light	6,401
tropism	6,365
photomorphogenesis	6,084
circadian rhythm	20,713
regulation of circadian rhythm	6,888
response to water deprivation	26,553
response to chitin	23,209
response to kamikinin	16,742
cellular response to starvation	6,828
reactive nitrogen species metabolic process	6,888
response to metal ion	6,759
regulation of response to osmotic stress	6,693
hypersensitive salinity response	6,342
response to cold	5,991

**H**

GO biological process complete	Enrichment
regulation of stomatal movement	9,275
defense response to bacterium	13,898
killing of cells of other organism	13,190
transmembrane receptor protein tyrosine kinase signaling	13,158
response to nematode	9,905
invertebrate immune response	9,362
immune effector process	9,216
regulation of ion transmembrane transport	9,191
cellular cation homeostasis	6,742
inorganic anion transport	6,476
transition metal ion homeostasis	6,360
metal ion transport	6,303
transcription, DNA-templated	93,048
protein autophosphorylation	21,878
RNA modification	13,500
oligopeptide transport	11,409
mRNA processing	10,840
translation	10,484
rRNA metabolic process	9,974
negative regulation of signal transduction	9,506
transmembrane transport	9,217
tRNA processing	8,018
ribosome biogenesis	7,766
chromatin organization	7,442
DNA metabolic process	7,181
protein targeting	7,021
establishment of protein localization to organelle	6,516
RNA splicing	6,432
nucleoside monophosphate metabolic process	6,180
trehalose biosynthetic process	6,092
negative regulation of transcription, DNA-templated	6,032
purine ribonucleotide metabolic process	6,020
protein import	5,958

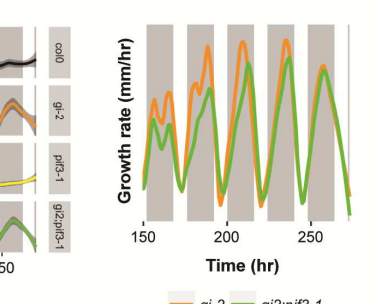
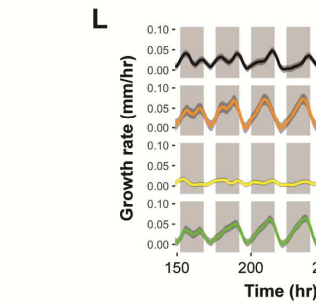
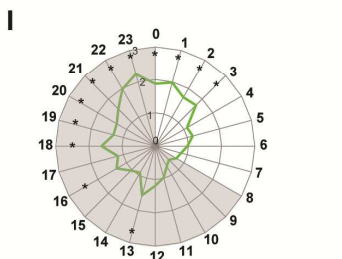
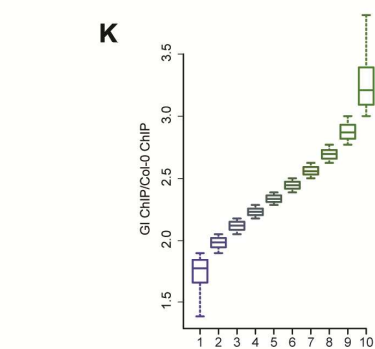
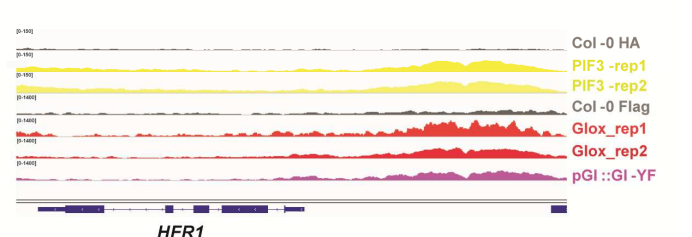


**Figure S4. GI and PIFs occupy the same genomic targets in a phase dependent pattern, Related to Figure 3**

(A) Protein accumulation pattern of GI-YPET-Flag (driven by an endogenous promoter fragment), PIF3-ECFP-HA (driven by an endogenous promoter fragment), and PIF5-HA (overexpressed) across SD photo-cycles. Protein levels were quantified relative to ACTIN levels.

(B and C) Time-course *in vivo* co-immunoprecipitation assays in *Arabidopsis* transgenic seedlings expressing GI-YPET-Flag and PIF3-ECFP-HA (driven by endogenous promoter fragments) (B, left panel), and GI-YPET-Flag and PIF5-HA (overexpressed) (B, right panel, and C) tagged protein versions.

(D) Overlap between peaks called in the different GI ChIP-seq biological replicates. Peaks identified in all three replicates were considered high confidence GI target sites (n=7365).

(E) Genomic annotation of a random permuted set of similar sample size to GI ChIP-seq peaks. Control to Figure 3D.

(F) Genomic annotation of PIF3 (n=7962) ChIP-seq peaks (left panel) compared to a random permuted set of similar sample size (right panel). The midpoint of the peaks was used for this analysis.

(G) Over-represented *cis* elements around the summit of PIF3 ChIP-seq peaks ( $\pm 100$  bp flanking region) in SD conditions.

(H) Heat map showing the GO term enrichment scores of genomic targets shared by GI and PIF3.

(I) Phase enrichment graph depicting the enrichment (count/expected) in the phase of peak expression of genomic targets shared by GI and PIF3 in SDs (\* $p < 0.01$ ). Day period is marked in white and night period in gray.

(J) Visualization of PIF3 and GI ChIP-seq data in the genomic region encompassing the *HFR1* locus.

(K) Boxplot of the signal from GI ChIP-seq peaks ranked by increasing signal and divided in 10 groups (deciles 1 to 10).

(L) Growth rate measurements (mm/h) of wildtype (Col-0), *gi-2*, *pif3-1*, and *gi-2;pif3-1* seedlings grown in SDs. Values represent mean  $\pm$  SEM (n=18-36). Time is expressed in hours after stratification. White and gray shadings represent day and night, respectively. The right panel shows the overlap of the growth rate measurement traces of *gi-2* and *gi-2;pif3-1* seedlings.



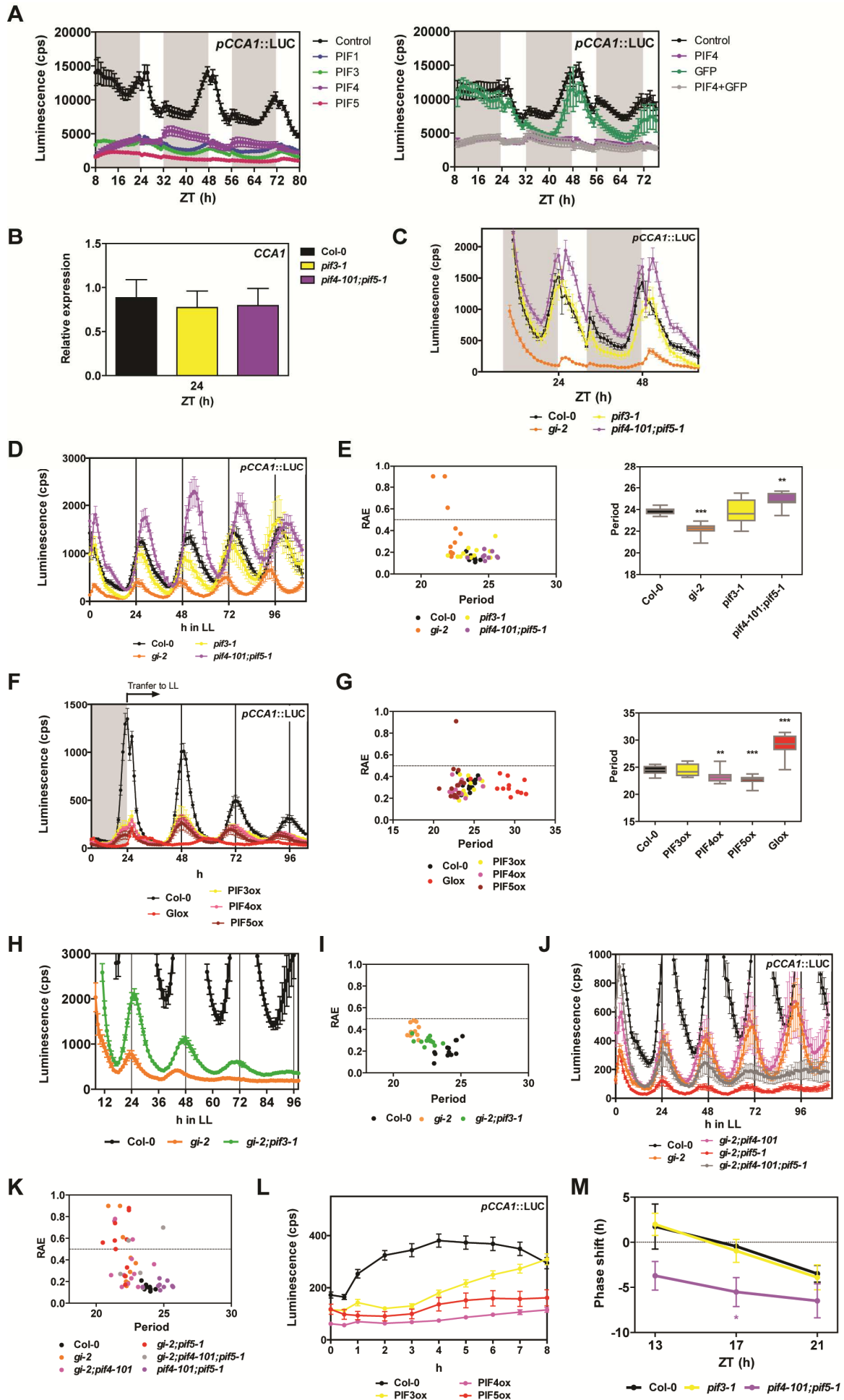


**Figure S5. GI modulation of light signaling affects circadian rhythms, Related to Figure 4**

(A) Transactivation assays in *N. benthamiana* leaves. Different effectors were co-expressed with the *pCCA1::LUC* reporter construct. Luminescence was measured 2 days post-infiltration in SD conditions. Results show mean  $\pm$  SEM (n=8).

(B) Relative expression of *CCA1* in the indicated backgrounds and ZTs in SDs (mean  $\pm$  SEM of 3 biological replicates).

(C) Bioluminescence analysis of *pCCA1::LUC* in seedlings in SD conditions. Values represent mean  $\pm$  SEM (n=12). White and gray bars represent day and night, respectively.

(D and F) Bioluminescence analysis of *pCCA1::LUC* in seedlings in constant light (LL). Values represent mean  $\pm$  SEM (n=24). Plants were entrained in SDs for 7 days.

(E and G) Left panels, period length estimations versus RAE of *pCCA1::LUC* in D and F as analyzed by FTT-NLLS. Right panels, period length estimations of *pCCA1::LUC* in D and F as analyzed by FTT-NLLS. Statistically significant differences between mean values by Student's *t*-test relative to the Col-0 control are shown (\*\* $p < 0.01$ , \*\*\* $p < 0.001$ ).

(H and J) Data shown in Figure 4E and G is re-plotted on a different scale for the y-axis.

(I and K) Period length estimations versus RAE of *pCCA1::LUC* data shown in Figure 4E and G as analyzed by FTT-NLLS.

(L) Bioluminescence analysis of *pCCA1::LUC* in 3 day old etiolated seedlings transferred to light (mean  $\pm$  SEM, n=12).

(M) Light-induced phase shifts of *pCCA1::LUC* expression plotted against the ZT at which the light pulse was given. Positive values represent phase advances and negative values, phase delays. Values represent mean  $\pm$  SEM (n=6).